

Preparation and Surface Modification of Electrospun Aligned Poly(butylene carbonate) Nanofibers

Meiling Shao, Lu Chen, Qing Yang

State Key Laboratory for Modification of Chemical Fibers and Polymer Materials, College of Material Science and Engineering, Donghua University, Shanghai 201620. People's Republic of China

Correspondence to: Q. Yang (E-mail: yangqing@dhu.edu.cn)

ABSTRACT: In this study, aligned poly(butylene carbonate) nanofibers were fabricated by electrospinning with a high-speed transfer roller as the receiving device. Cold plasma treatment technology was applied to improve its hydrophilicity and activity to expand its application in biological materials. The morphology of the fibers was investigated with scanning electron microscopy. X-ray diffraction was used to research the impact of the rotation speed on the crystallization and orientation degree of the crystals. The tensile properties of the materials were evaluated by a universal tester. The surface properties of the fibers pretreated by Helium (He) and those grafted with gelatin were evaluated with water contact angle measurement and X-ray photoelectron spectroscopy. The experimental results indicate that the order degree of fibers, crystallinity, and orientation of the crystalline region, including the mechanical properties, all increased correspondingly with the rotation speed. After plasma pretreatment, the hydrophilicity was improved significantly, and the grafting reaction was realized successfully. © 2013 Wiley Periodicals, Inc. *J. Appl. Polym. Sci.* 130: 411–418, 2013

KEYWORDS: biomaterials; crystallization; electrospinning; grafting; mechanical properties

Received 29 November 2012; accepted 27 January 2013; published online 18 March 2013

DOI: 10.1002/app.39103

INTRODUCTION

In the 21st century, biomaterials that can be used to diagnose, treat, repair, or replace worn tissue or enhance their functions have become an important branch of biomedicine.¹ These materials must be complete with excellent biological replaceability (mechanical properties, functionality) and biocompatibility for long-term contact with the body, blood, and fluids or even permanent *in vivo* implantation.² Aliphatic polyesters are a class of polymers that have been widely investigated for a variety of biomedical applications.³ Members of this family, such as poly(lactic acid), poly(glycolic acid), and polycaprolactone (PCL), have been approved by the U.S. Food and Drug Administration.⁴ Although among these, PCL, with its excellent mechanical properties and processability because of special carbon chain structures, has been a research hotspot for decades,⁵ the problem of a slow degradation rate (a degradation cycle of 2–3 years *in vivo*) still limits its application today.^{6,7}

Recently, it has become important to endow materials with excellent and diverse performances by molecular design in the biomaterials field. Poly(butylene carbonate) (PBC), which is another important member of the aliphatic polyester family, is a kind of new biomaterial obtained via a successive two-step polycondensation.^{8,9} Apart from the methylene that is connected

with the carbonyl in the backbone chain being replaced by an oxygen atom, the structural formula of PBC is similar to that of PCL.¹⁰ So PBC possesses excellent impact resistance and satisfactory tensile strength just as PCL because of the flexibility of its chains, whereas the degradation rate is much faster with the replaced oxygen atom, with a degradation cycle of half a year.¹⁰

Recently, it was discovered that a nanoscale fiber diameter can be achieved by electrospinning.^{11,12} Ultrafine fibers with a high porosity and large surface area could imitate the natural extracellular matrix on the nanoscale and could be used as a porous scaffold to promote cell migration and proliferation.^{13,14} In tissue engineering, the hydrophilicity of materials is an important factor in evaluating the adhesion of cells. Although the hydrophilicity of fibers with a large porosity will be improved, the fibers mat's surface will still be hydrophobic because of the nature of most synthetic polymers, including PBC. Plasma treatment is an effective method for improving the hydrophilic properties of a material's surface; during the process, part of the ionized gas particles bombard the surface to introduce functional groups as $-\text{COOH}$, $-\text{NH}_2$, and $-\text{OH}$.^{15,16} Then, other molecules or groups are grafted to the surface by these active groups to obtain the desired properties.^{17,18}

To the best of our knowledge, little attention has been paid to PBC so far; this may be because of its unavailability. In this study, PBC was chosen to prepare aligned nanofibers by electrospinning, and then, the surface activity was pretreated with cold plasma. Gelatin was introduced onto the surface of the pretreated fibers to increase the biocompatibility of the materials. The basic performances of the nanofibers were investigated, together with the surface properties of the fibers before and after modification.

EXPERIMENTAL

Materials

PBC, with a number-average molecular weight of 7.0×10^5 Da and a polydispersity index of 1.77, was provided by Sanfangxiang Group Co., Ltd. (Jiangsu, China). The samples were cleaned with deionized water and dried at room temperature before use. Formic acid (FA) was purchased from National Pharmaceutical Group Chemical Reagent Co., Ltd. Gelatin for surface grafting was obtained from Shanghai Fankelbio Science & Technology Co., Ltd.

Preparation of the Aligned PBC Nanofibers

The aligned nanofibers were fabricated by electrospinning with a rotating drum as a collector. In brief, a polymer solution (25% (w/v)) was prepared by dissolution in a given amount of PBC in FA; this was stirred at room temperature for 3 h. The solution was injected into a 5-mL glass syringe, and then, the syringe was placed in a boost pump with a boost speed of 0.4 mL/h to prepare the solution for injection. A high voltage generated by a high-voltage power supply was applied to the syringe needle, and the aligned fibers were received on the rotating drum. During the experiment, the voltage was maintained at 18 kV, the distance between the needle and the collector was 20 cm, and the rotation speed of the collector was 1000–12,000 rpm and could be controlled by a transducer.

Plasma Pretreatment and Surface Grafting

The aligned nanofiber mats were put into a cylindrical vacuum chamber of a cold plasma processor; we evacuated the chamber until the pressure dropped down to 0 Pa and purged it with reactant He gas for 10 min. Then, He was fed into the chamber constantly to maintain the working pressure at 20 Pa under the conditions of a discharge power of 20–100 W. The samples were treated for 30–150 s. Then, some of the pretreated samples were soaked in a gelatin solution (10 wt %) overnight to allow the reaction to proceed to completion. After the sample was placed in deionized water and cleaned ultrasonically three times (20 min) at 35°C to dissolve the absorbed gelatin, the products of the graft were soaked in deionized water overnight to thoroughly remove the unreacted gelatin and were then dried at room temperature.

Scanning Electron Microscopy

PBC nanofiber mats prepared at different rotation speeds were observed under scanning electron microscopy (JSM-56000LV, Japan) operated at 10 kV after they were sputtered with gold. Images of the aligned fibers were taken to observe the morphology and microstructure of the fibers. The fiber diameter and angular deviation from orientation were obtained by analysis of

the micrographs with the image analysis software ImageJ version 1.37.

Porosity Measurement

The porosity was measured by the following method: a certain area of wet nanofiber mats were clipped, and excess water on the surface was wiped off with filter papers; the sample was then weighed (W_1). W_2 is the weight of the mats after drying in a vacuum oven to a constant weight. Then, the porosity (P_r) was calculated according to the following equation:

$$P_r = \frac{W_1 - W_2}{\rho AL_d} \times 100\%$$

where A is the area of the fiber mats (cm^2), L_d is the thickness of the mats (cm), and ρ is the density of water (1 g/cm^3).

Every sample was tested five times, and we then took the average.

Wide-Angle X-ray Diffraction (XRD) Analysis

The crystal structures and orientation degree of the crystalline region were measured by a wide-angle X-ray diffractometer (D/max-2550 PC, Japan). Crystal structures were detected by a reflection method. The samples were cut into powders and then pressed into the sample holder; the orientation degrees were measured by a transmission method, and the fiber mats were scanned along the fiber orientation. The test conditions were as follows: the samples were scanned at $2\theta = 5\text{--}80^\circ$, and the operating voltage and current were 40 kV and 150 mA, respectively. The radiation was Ni-filtered Cu K α radiation with a wavelength of 1.54056 Å, and the scanning speed was 5°/min.

Tensile Properties Test

Electrospun fiber mats prepared at different rotation speeds were cut into $8 \times 1 \text{ cm}^2$ samples. The thickness of the mats was determined by a thickness gauge to obtain the sections. The samples were fixed in the clamp of the universal testing machine with a loading velocity of 15 mm/min. Five square strips of each sample were tested, and we then took the average.

Water Contact Angle Measurement

The hydrophilicity values of the samples before and after modification were tested by a Micro Optical Angle Measurement (OCA40, GER). An amount of 2 μL of deionized water was dropped on the surface of the samples at an injection speed of 0.52 $\mu\text{L/s}$.

X-ray Photoelectron Spectroscopy (XPS) Analysis

The surface elements and content of the electrospun fiber mats before and after modification were characterized with XPS (ESCALAB 200R, United Kingdom). The test conditions were as follows: Al K α X-rays (300 W) were used as the excitation source with an optimum energy resolution of 0.47 eV.

RESULTS AND DISCUSSION

Surface Morphologies of the Aligned Nanofibers

Early in the 1990s, when the electrospinning technique was used in the preparation of polymer nanofibers, Doshi and Reneker¹⁹ proposed that parallel nanofibers could be obtained by a high-speed rotating drum as a collecting device. Theoretically, when

the deposition speed on the receiving device is close to the rotation speed, the uniaxially oriented fibers can be received. So it can be drawn, and the arrangement of the fibers is the interaction of the roller speed and jet speed. However, the jet is not stretched at a constant speed in the electrospinning process, and the speed is hard control by anthropic factors, so it becomes very critical to adjust the rotation speed. In this study, we adopted linear velocity to characterize the rotation speed to study the impact on the fibers' arrangement.^{20,21}

As shown in Figure 1 about the morphologies of the PBC nanofibers obtained with rotation speeds from 3 to 10 m/s, we directly observed that the order degree of the arranged fibers increased significantly. Meanwhile, the fibers' average diameters decreased gradually from about 350 nm at 3 m/s to around 220 nm at 9 m/s (from Figure 2), the diameter distribution was more uniform, and the surface of the fibers was smoother. As shown in the histogram insert Figure 1, the angle of the particles was more concentrated around 90° at 9 m/s. The angle was the included angle between the principle elliptical axis of the particle and the horizontal direction, so it could be used to quantitatively analyze the fiber arrangement. When the angles were concentrated around 90°, we obtained the best aligned fibers. Throughout the spinning process, the jet mainly deposited on the front of the roller when the rotation speed was low; this made part of the fibers distribute desultorily or even stick together, which led to an order degree was not high. As the speed increased, the air convective motion around the roller was

intensified; by the role of convection, the jet bypassing the roller deposited on the back of it and wound like an ordinary winding process. What is more, the thinness of the fibers was also such that the fibers were further stretched during the winding process. However, when the speed exceeded 9 m/s, the order degree decreased, and the diameters thickened obviously because of the overdramatic convection that caused a change in the fibers' trajectory around the roller to make the chaotic fibers deposit directly without winding. The other part of the fibers, which were overstretched because of the excessive speed, were slightly deformed or even broken, and this caused nonuniformity in the diameter distribution.

In most application process, biomaterials should have a certain porosity and permeability to ensure the smooth process of substance transfer, such as the absorption of nutrients and the exportation of waste products. Fiber mats are usually porous for the position of fibers obtained by the randomly distributed electrospinning. The porosity of random PBC fiber mats received at 0 m/s was about 84.42%, and the ordered fiber mats' porosity at different rotation speeds is shown in Figure 2. As shown, the regularity of the fibers led to a reduction in the porosity with increasing speed; it reached a minimum value of 68.83% at 9 m/s, and this was consistent with the arrangement of the fibers.

Crystalline Properties of the Aligned Nanofibers

The crystallinity of the aligned fibers characterized by XRD is shown in Figure 3. It can be seen there were three sharp

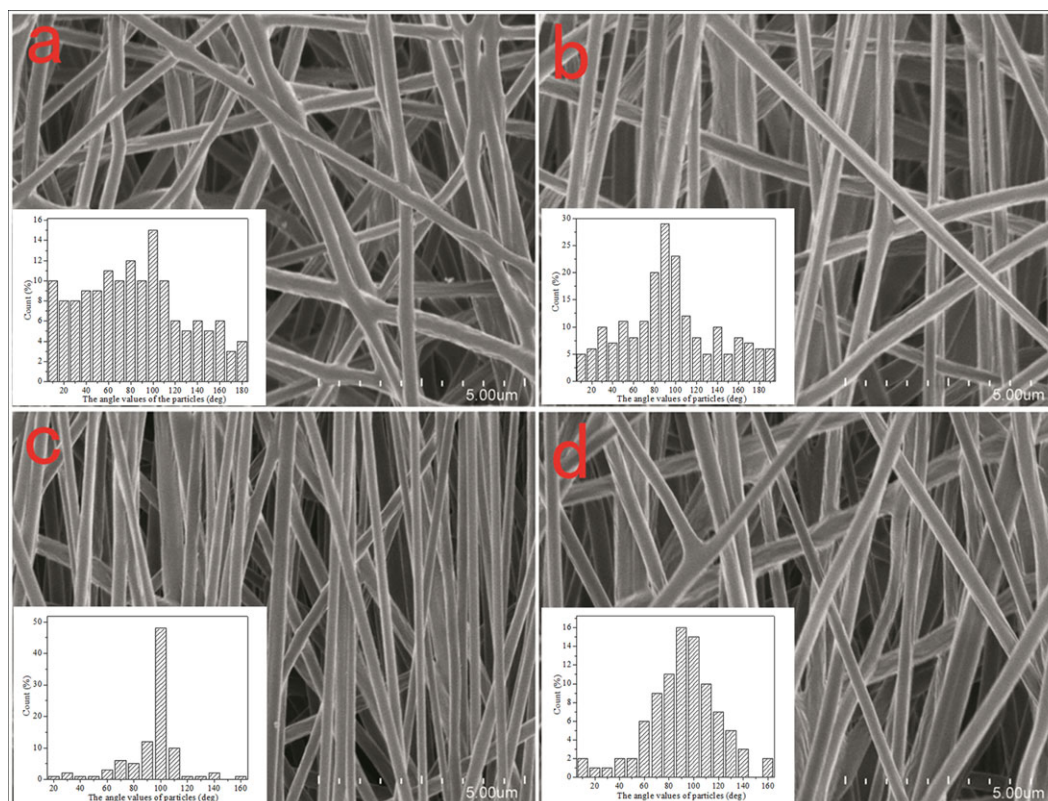


Figure 1. Micromorphologies and particle distribution histogram of aligned PBC nanofibers collected at different rotation speeds: (a) 3, (b) 6, (c) 9, and (d) 10 m/s. [Color figure can be viewed in the online issue, which is available at wileyonlinelibrary.com.]

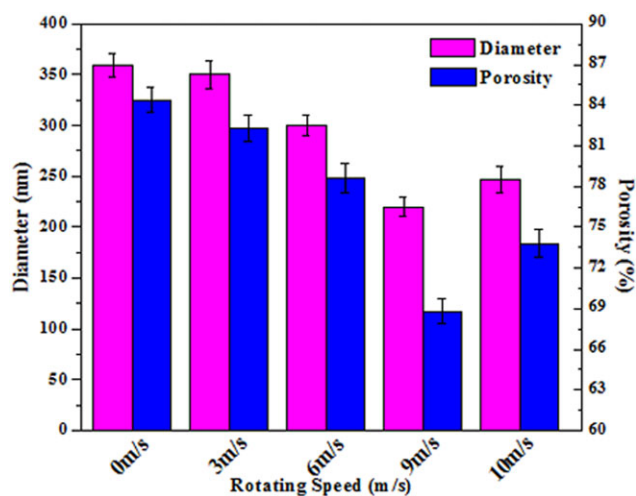


Figure 2. Diameter and porosity of the aligned PBC nanofibers collected at different rotation speeds. [Color figure can be viewed in the online issue, which is available at wileyonlinelibrary.com.]

crystalline diffraction peaks in the spectrograms of the fibers with different rotation speeds at $2\theta = 16.34, 20.76,$ and 22.66° ; these correspond to the [101], [020], and [110] planes, respectively. With increasing rotation speed, the narrowing and sharpening of the three peaks indicated that the degree of crystallinity increased significantly (from 29.16 to 46.81% according to the data in Table I). According to the literature on aliphatic polycarbonate, there are a large number of potential nucleation mechanisms and immature crystals that could cause the crystallization of PBC, which is regarded as a semicrystalline polymer, to be very slow.²² From the preceding analysis, the stretching of the fibers occurred not just in the electric field but in the winding process, and the succeeding stretching became intense with increasing rotation speed. As we know, stretching promotes the orientation of the molecular chains, thereby inducing the formation and growth of nuclei. As shown by the data in Table I,

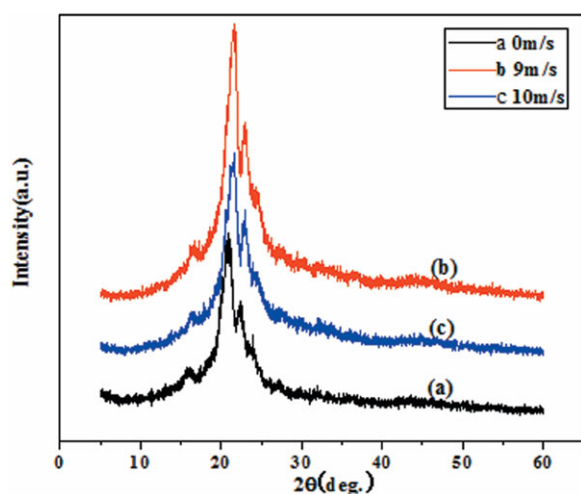


Figure 3. XRD spectra of the aligned PBC nanofibers collected at different rotation speeds: (a) 0, (b) 9, and (c) 10 m/s. [Color figure can be viewed in the online issue, which is available at wileyonlinelibrary.com.]

Table I. Grain Size, Crystallinity, and Orientation Degree of the Aligned PBC Nanofibers Collected at Different Rotation Speeds

| Sample | Linear velocity (m/s) | [101] (Å) | [020] (Å) | [110] (Å) | Crystallinity (%) | Orientation degree (%) |
|--------|-----------------------|-----------|-----------|-----------|-------------------|------------------------|
| a | 0 | 251 | 118 | 177 | 29.16 | 0 |
| b | 3 | 205 | 122 | 167 | 37.86 | 55.43 |
| c | 6 | 118 | 109 | 149 | 42.19 | 68.75 |
| d | 9 | 122 | 103 | 154 | 46.81 | 83.66 |
| e | 10 | 164 | 113 | 167 | 44.59 | 79.28 |

the grain sizes of the three characteristic crystal planes were 251, 118, and 177 Å at 0 m/s; they all decreased significantly with increasing speed. For one thing, more nuclei were generated; for another, the fiber diameters decreased when the crystal growth space was limited by stretching. When the speed was up to 10 m/s, because the grain size of the nonwound fibers deposited on the surface was still large, the results showed a relative increase.

Orientation Degree of Crystal Analysis

Generally speaking, by a simple electrostatic spinning apparatus, a Taylor cone is formed from polymer droplets in the nozzle by an electric field force, so submicrometer or nanoscale fibers are aggregated by disordered fibers, which cause the orientation of the molecule to be hidden. By the use of high-speed rotary receiving means, the arrangement and direction of the fibers can be controlled with the physical extension effect of jet flow resulting from a high rotation speed; meanwhile, the molecular orientation also became distinct. The crystalline region orientation of the PBC aligned fibers obtained under different speeds is shown in Figure 4. At a speed of 0 m/s, the orientation degree of the fibers was measured to be 0. When the speed was

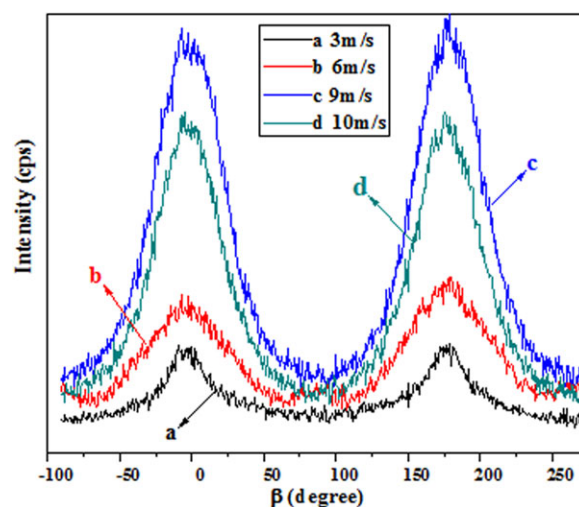


Figure 4. XRD patterns for the crystalline orientation of the aligned PBC nanofibers collected at different rotation speeds: (a) 3, (b) 6, (c) 9, and (d) 10 m/s. [Color figure can be viewed in the online issue, which is available at wileyonlinelibrary.com.]

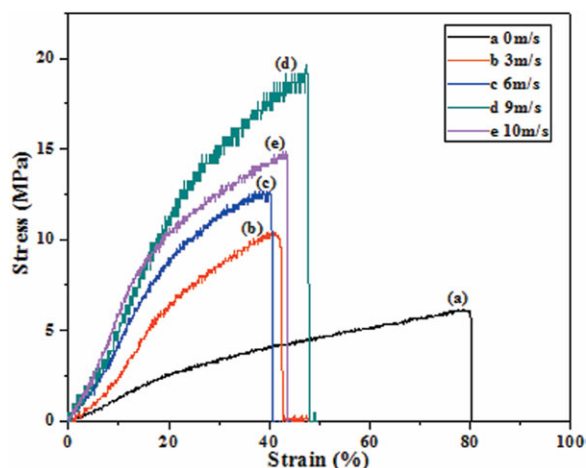


Figure 5. Stress–strain curves of the aligned PBC nanofiber mats: (a) 0, (b) 3, (c) 6, (d) 9, and (e) 10 m/s. [Color figure can be viewed in the online issue, which is available at wileyonlinelibrary.com.]

increased from 3 to 10 m/s, the orientation degree also grew correspondingly from 55.43 to 83.66%, as shown in Table I. In addition, when the speed exceeded the critical value of 9 m/s, the fibers became curving and fractured, so the orientation degree tended to decline. This further proved that the best aligned fibers could be obtained only at the appropriate speed.

Tensile Properties of the Aligned Nanofiber Mats

As shown in Figure 5, in the stress–strain curves of the aligned fiber mats obtained at different rotation speeds, we could see that the tensile properties of the mats improved markedly with increasing speed. The tensile strength of the fibers with random arrangement was very low at about 6.17 MPa; the data are listed in Table II. This suggests that the mats were endowed with poor properties of softness and friability. However, the data gradually increased after the fiber order degree increased with increasing rotation speed. The value grew to 19.12 MPa when the speed was increased to 9 m/s. According to the previous analysis, from the macroscopic view, the increase in the rotation speed promoted the arrangement of fibers. From the microscopic view, it was also encouraged by the orientation of the molecular chain and also the increase in crystallinity and the reduction in grain size. These combined effects drastically improved the tensile strength and elasticity modulus along the arrangement direction of the fibers. Although when the speed was faster than 9 m/s, the mechanical strength decreased remarkably because of the decrease in the arrangement order and crystallinity and the

partial breakage of fibers due to the excessive rotation speed. The same trend was also evident for the elasticity modulus.

Surface Hydrophilic Surface Testing of the Pretreated Fiber Mats

The hydrophilicity is the key factor affecting the initial behavior between biological materials and cells,²³ and it can be an indicator of the interactions. Materials with a good hydrophilicity can promote the adhesion of cells. Contact angle measurement is a common method for characterizing the hydrophilicity, and the hydrophobicity is relatively strong when the angle of the droplet on the material's surface is greater than 90°; on the contrary, the material is hydrophilic.

PBC is a typical hydrophobic material, and it had a contact angle of about 120° on the untreated fiber mats. After plasma pretreatment, the water droplet spread out rapidly when it touched the surface until the angle decreased to 0°. This was just like the change showed by the insets in Figure 6(B). This suggested that there was a significant improvement in the hydrophilicity associated with the bond breaking and generation of hydrophilic groups that strengthened the polarity of the surface in the treatment process. In this study, the dynamic contact angles were measured to analyze the impact of different processing powers and times on the hydrophilicity: the faster the angles changed, the better the hydrophilicity was, and vice versa.

Dynamic changes in the contact angles on the pretreated fiber mats with different processing powers are shown in Figure 6(A). They all decreased to 0° quickly (within 20 s). With the increase in powers, the rate of change gradually accelerated, but when the power was more than 80 W, it actually slowed. The effects of the plasma treatment on the polymer surface were mainly of three types: etching (physical change), surface crosslinking, and chemical modification. When the discharge power was excessive, the etching effect increases over other effects and led to a loss of the hydrophilic groups that were introduced. The hydrophilic layer was damaged, so the angle change rate deteriorated at 100 W. As shown in Figure 6(B), a change in the processing time also showed similar results. By comparison, the mats obtained at 80 W maintained for 120 s displayed the optimal hydrophilicity, and this value of the parameter was chosen for surface grafting.

Surface Elemental Analysis of the Modified Fiber Mats

XPS was carried out to characterize the chemical composition, structures, and combination of the surface before and after modification; it can analyze all elements except hydrogen. During the analysis by XPS, first of all, full scanning was used to

Table II. Relationship of the Mechanical Properties and Rotation Speed

| Sample | Linear velocity (m/s) | Tensile strength (MPa; error) | Elasticity modulus (GPa; error) | Elongation at break (%; error) |
|--------|-----------------------|-------------------------------|---------------------------------|--------------------------------|
| a | 0 | 6.17 (3.26%) | 0.04 (0.91%) | 80.33 (6.23%) |
| b | 3 | 10.41 (3.43%) | 0.35 (1.38%) | 42.64 (4.32%) |
| c | 6 | 12.64 (3.21%) | 0.46 (0.74%) | 40.57 (5.36%) |
| d | 9 | 19.12 (3.33%) | 0.57 (1.69%) | 47.86 (4.18%) |
| e | 10 | 14.86 (2.62%) | 0.43 (1.41%) | 43.64 (3.04%) |

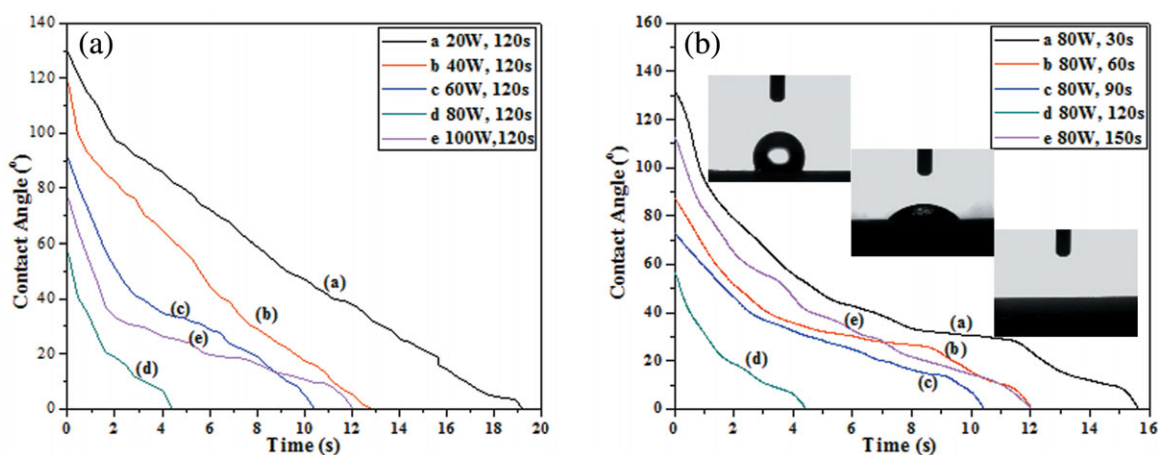


Figure 6. Changes in the hydrophilicity after plasma pretreatment: (a) different processing powers and (b) different processing times. [Color figure can be viewed in the online issue, which is available at wileyonlinelibrary.com.]

identify the elements present in the surface of the fibers, as shown in Figure 7. From the figure, we can see that there were C1s and O1s peaks on all of the samples at 285 and 530 eV around,¹⁶ but after plasma pretreatment, the oxygen peak became strong, and the carbon peak weakened. An obvious nitrogen peak that arose at about 420 eV on the gelatin-grafted fibers' spectrogram illustrated that gelatin was successfully introduced onto the surface of the fibers to form bonds, such as amide bonds.

The percentage and ratio of each element of the samples based on XPS quantitative analysis are shown in Table III. The O/C ratio was significantly improved on the pretreated fibers, from 37.49 to 57.78%. This was associated with the formation of

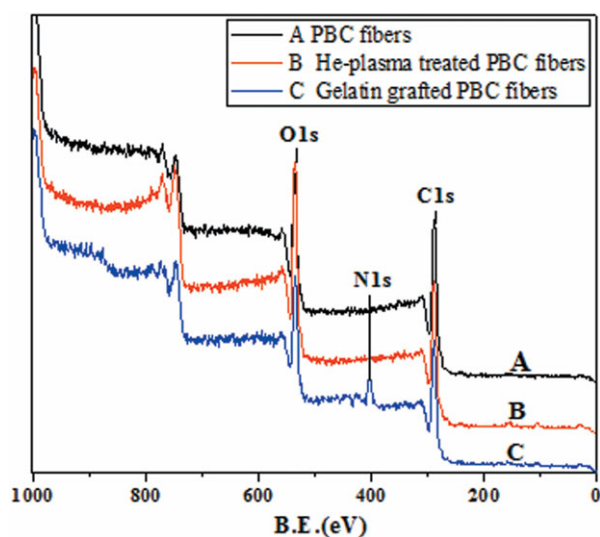


Figure 7. XPS survey scan spectra of the PBC fibers before and after treatment: (A) untreated PBC fibers, (B) He-plasma-pretreated PBC fibers (80 W and 120 s), and (C) gelatin-grafted PBC fibers. B. E. = binding energy. [Color figure can be viewed in the online issue, which is available at wileyonlinelibrary.com.]

oxygen functional groups, such as carboxyl groups ($-\text{COOH}$). Energy was transmitted to the surface by the metastable chemical group with a relatively high energy when He plasma acted on the surface, whereas the collision of electrons in the plasma also delivered energy to form unsaturated bonds. Then the sample was subsequently exposed to air to incorporate oxygen, and this resulted in the oxygen content significantly increasing (from 27.27 to 36.62%). After pretreatment, gelatin was grafted onto the fibers, and this led to the introduction of a large amount of nitrogen (content = 10.70%). This indicated that the amino groups of gelatin reacted with the carboxyl groups generated by pretreatment to realize the grafting reaction.

Then narrow scanning of the C1s peak was carried out to determine the elemental combination of the modified fibers. Figure 8(A–C) shows the spectrogram of the C1s after peak separation and fitting. The peaks located at the 284.2, 286.0, and 288.4 eV represented the $-\text{C}-\text{C}-$, $-\text{C}-\text{O}-$, and $-\text{C}(=\text{O})-$ bonds, respectively.²⁴ On closer examination, the integral peak areas of the $-\text{C}-\text{O}-$ and $-\text{C}(=\text{O})-$ bonds increased visibly after pretreatment. It was evident that there were more polar groups bonded on the surface; the effect was more obvious after grafting. As shown in Table III, there was a clear change in all of the carbon-containing functional groups. These results indicate that during the treatment process, the $-\text{C}-\text{C}-$ bond broke down to form $-\text{C}-\text{O}-$ and $-\text{C}(=\text{O})-$ bonds or other polar groups; this also made the surface activity much better.

Figure 8(D) shows the N1s spectra after the swarming and fitting of the grafted fibers. The peaks at 399.4 and 401.5 eV represented $-\text{N}-\text{C}-/-\text{N}=\text{C}-$ and $-\text{N}-\text{O}-$, respectively,²⁵ and the corresponding proportions were 69.96 and 30.04% (from Table III). This further confirmed that the nitrogen introduced mainly existed in the form of amide bonds.

CONCLUSIONS

In this study, we found that the best rotation speed to prepare aligned PBC nanofibers was 9 m/s. The obtained fibers had the best order degree. Meanwhile, the fiber surface was smooth, and

Table III. Quantitative Elementary and Bond Analysis of the Untreated, He-Treated, and Gelatin-Grafted Samples as Measured by XPS

| Sample | Atomic fraction (%) | | | Atomic ratio (%) | | Correlative functional groups fraction (%) | | | | |
|---------------------------------|---------------------|-------|-------|------------------|-------|--|---------------------|-----------------------|--------------------------|---------------------|
| | C | O | N | O/C | N/C | -C-C- (284.2 eV) | -C-O- (286.0 eV) | -C(=O)- (288.4 eV) | -N-C/-N=C- (399.4 eV) | -N-O- (401.5 eV) |
| PBC fibers | 72.73 | 27.27 | — | 37.49 | — | 75.23 | 21.53 | 3.24 | — | — |
| He-plasma-pretreated PBC fibers | 63.38 | 36.62 | — | 57.78 | — | 66.98 | 27.26 | 5.67 | — | — |
| Gelatin-grafted PBC fibers | 60.83 | 28.47 | 10.70 | 46.80 | 17.59 | 58.46 | 35.43 | 6.11 | 69.96 | 30.04 |

the diameters were uniform at about 220 nm, and the porosity decreased to a minimum value of 68.83%.

During the process of preparing the aligned PBC nanofibers, the order degree of fibers, the crystallinity, and the orientation of crystalline region, including mechanical strength, all increased correspondingly with increasing rotation speed, and they all ran up to a maximum at 9 m/s and then started to decrease. Among the rest, the tensile strength increased up to 19.12 MPa three times as random fibers.

After plasma pretreatment, the hydrophilicity of the aligned fiber mats improved significantly. The dynamic contact angle data indicated that the completely hydrophobic surface changed into a hydrophilic one. By comparison, the mats that were obtained at 80 W and maintained for 120 s had the optimal hydrophilicity.

The fiber mats were then immersed in a gelatin solution for grafting after pretreatment. The XPS results show that some oxygen was introduced onto the surface of the pretreated

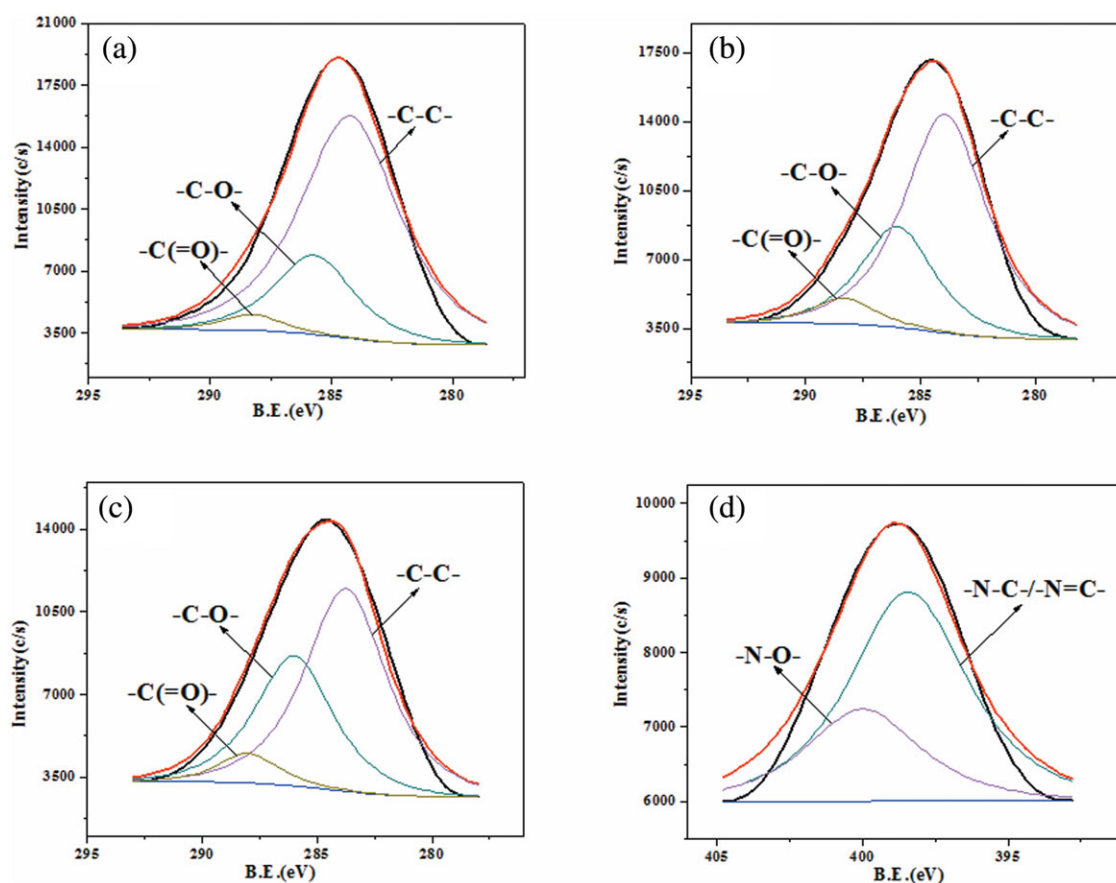


Figure 8. XPS C1s and N1s spectra of samples before and after treatment: (a) C1s of the original fibers, (b) C1s of the He-plasma-pretreated fibers, (c) C1s of the gelatin-grafted fibers, and (d) N1s of the gelatin-grafted fibers. [Color figure can be viewed in the online issue, which is available at wileyonlinelibrary.com.]

samples on subsequent exposure to air (with the atomic fraction rising from 27.67 to 36.62%); the amide bond was formed on the surface of the mats grafted with gelatin, as proven by the obvious nitrogen peak in the XPS spectrogram.

ACKNOWLEDGMENTS

This research was financially supported by State Key Laboratory for Modification of Chemical Fibers and Polymer Materials (contract grant number LZ0902).

REFERENCES

1. Nair, L. S.; Laurencin, C. T. *Prog. Polym. Sci.* **2007**, *32*, 762.
2. He, W.; Ma, Z.; Yong, T.; Teo, W. E.; Ramakrishna, S. *Biomaterials* **2005**, *26*, 7606.
3. Martino, S.; D'Angelo, F.; Armentano, I.; Kenny, J. M.; Orlacchio, A. *Biotechnol. Adv.* **2012**, *30*, 338.
4. Jiang, X.; Lim, S. H.; Mao, H.; Chew, S. Y. *Exp. Neurol.* **2010**, *223*, 86.
5. Croisier, F.; Duwez, A. S.; Jérôme, C.; Léonard, A. F.; van der Werf, K. O.; Dijkstra, P. J.; Bennink, M. L. *Acta Biomater.* **2012**, *8*, 218.
6. Kweon, H.; Yoo, M. K.; Park, I. K.; Kim, T. H.; Lee, H. C.; Lee, H.; Oh, J.; Akaike, T.; Cho, C. *Biomaterials* **2003**, *24*, 801.
7. Sun, H.; Mei, L.; Song, C.; Cui, X.; Wang, P. *Biomaterials* **2006**, *27*, 1735.
8. Wang, J.; Zheng, L.; Li, C.; Zhu, W.; Zhang, D.; Xiao, Y.; Guan, G. *Polym. Test* **2012**, *31*, 39.
9. Li, J. Y.; Mai, Y. Y.; Yan, D. Y.; Chen, Q. *Colloid Polym. Sci.* **2003**, *281*, 267.
10. Zhu, W.; Huang, X.; Li, C.; Xiao, Y.; Zhang, D.; Guan, G. *Polym. Int.* **2011**, *60*, 1060.
11. Ghasemi-Mobarakeh, L.; Prabhakaran, M. P.; Morshed, M.; Nasr-Esfahani, M.; Ramakrishna, S. *Biomaterials* **2008**, *29*, 4532.
12. Bhardwaj, N.; Kundu, S. C. *Biotechnol. Adv.* **2010**, *28*, 325.
13. Huang, W.; Shi, X.; Ren, L.; Du, C.; Wang, Y. *Biomaterials* **2010**, *31*, 4278.
14. Ramakrishna, S.; Jose, R.; Archana, P. S.; Nair, A. S.; Balamurugan, R.; Venugopal, J.; Teo, W. E. *J. Membr. Sci.* **2010**, *45*, 6283.
15. Messina, G. M. L.; Satriano, C.; Marletta, G. *Colloids Surf. B* **2009**, *70*, 76.
16. Kull, K. R.; Steen, M. L.; Fisher, E. R. *J. Membr. Sci.* **2005**, *246*, 203.
17. Ferreira, B. M. P.; Pinheiro, L. M. P.; Nascente, P. A. P.; Ferreira, M. J.; Duek, E. A. R. *Mater. Sci. Eng. C* **2009**, *29*, 806.
18. Bodas, D.; Khan-Malek, C. *Microelectron. Eng.* **2006**, *83*, 1277.
19. Doshi, J.; Reneker, D. H. *J. Electrostat.* **1995**, *35*, 151.
20. Lee, J. Y.; Bashur, C. A.; Goldstein, A. S.; Schmidt, C. E. *Biomaterials* **2009**, *30*, 4325.
21. Lee, K. H.; Kim, H. Y.; Khil, M. S.; Ra, Y. M.; Lee, D. R. *Polymer* **2003**, *44*, 1287.
22. Qiu, Z.; Miao, L.; Yang, W. *J. Polym. Sci. Part B: Polym. Phys.* **2006**, *44*, 1556.
23. Kim, C. H.; Khil, M. S.; Kim, H. Y.; Lee, H. U.; Jahng, K. Y. *J. Biomed. Mater. Res. Part B: Appl. Biomater.* **2006**, *78*, 283.
24. Chen, J.; Su, C. *Acta Biomater.* **2011**, *7*, 234.
25. Li, X.; Zhu, L.; Xu, Y.; Yi, Z.; Zhu, B. *J. Membr. Sci.* **2011**, *374*, 33.